

Broad-band efficiency calibration of ITER bolometer prototypes using Pt absorbers on SiN membranes

H Meister, M Willmeroth,^{1, a)} D Zhang,² and , A Gottwald, M Krumrey, F Scholze³

¹⁾*Max-Planck-Institut für Plasmaphysik (IPP), EURATOM Association,
Boltzmannstr. 2, 85748 Garching, Germany*

²⁾*Max-Planck-Institut für Plasmaphysik (IPP), EURATOM Association,
Teilinstitut Greifswald, Wendelsteinstraße 1, 17491 Greifswald,
Germany*

³⁾*Physikalisch-Technische Bundesanstalt (PTB), Abbestraße 2-12, 10587 Berlin,
Germany*

The energy resolved efficiency of two bolometer detector prototypes for ITER with 4 channels each and absorber thicknesses of $4.5\,\mu\text{m}$ and $12.5\,\mu\text{m}$, respectively, has been calibrated in a broad spectral range from $1.46\,\text{eV}$ up to $25\,\text{keV}$. The calibration in the energy range above $3\,\text{eV}$ was performed against previously calibrated silicon photodiodes using monochromatized synchrotron radiation provided by five different beamlines of PTB at the electron storage rings BESSY II and Metrology Light Source in Berlin. For the measurements in the visible range a set-up was realised using monochromatized halogen lamp radiation and a calibrated laser power meter as reference. The measurements clearly demonstrate that the efficiency of the bolometer prototype detectors in the range from $50\,\text{eV}$ up to $\approx 6\,\text{keV}$ is close to unity; at a photon energy of $20\,\text{keV}$ the bolometer with the thick absorber detects 80% of the photons, the one with the thin absorber about 50%. This indicates that the detectors will be well capable of measuring the plasma radiation expected from the standard ITER scenario. However, a minimum absorber thickness will be required for the high temperatures in the central plasma. At $11.56\,\text{keV}$ the sharp Pt- L_3 absorption edge allowed to cross-check the absorber thickness by fitting the measured efficiency to the theoretically expected absorption of X-rays in a homogeneous Pt-layer. Furthermore, below $50\,\text{eV}$ the efficiency first follows the losses due to reflectance expected for Pt, but below $10\,\text{eV}$ it is reduced further by a factor of 2 for the thick absorber and a factor of 4 for the thin absorber. Most probably, the different histories in production, storage and operation led to varying surface conditions and additional loss channels.

PACS numbers: 07.57.Kp, 06.20.fb, 28.52.-s, 52.70.-m

^{a)}Electronic mail: meister@ipp.mpg.de

I. INTRODUCTION

In fusion devices the total plasma radiation, part of the overall energy balance, is determined by the bolometer diagnostic. The bolometer detector type being used most commonly is the miniaturised metal resistor bolometer¹, which was also chosen as the ITER reference detector type². In view of ITER, R&D efforts have been started to develop a radiation resistant detector suitable for the operation under the harsh environmental conditions expected. So far, these efforts resulted in a detector prototype based on the design of the commonly used foils with Au-absorber on a mica or kapton substrate^{1,3-5} (e.g.), but now using Pt-absorber on SiN-membranes with Pt-resistors on the back side for each of the 4 channels as Pt has a 10 times lower cross section for neutron capture than Au and SiN is one of the ceramics shown to be irradiation tolerant⁶. These prototypes could be characterised under laboratory conditions and operated successfully in ASDEX Upgrade since 2009^{7,8}. Latest developments led to a version featuring an up to $12.5\mu\text{m}$ thick absorber suitable for the detection of high energy photons as they are expected from the centre of the ITER plasma with its high electron temperatures.

The spatial distribution of the plasma radiation density can be determined by applying tomographic reconstruction methods on the measurements of many lines-of-sight (LOS)⁹. This profile is an important input for transport studies and the characterisation of advanced plasma scenarii which rely on strongly radiating plasma boundaries to reduce the thermal loads on plasma facing components¹⁰. The most accurate reconstruction results in support of these studies can be achieved only if the spectral characteristics of the energy absorption of the bolometer detectors are known. Additionally, the accuracy of the evaluated total radiative loss P_{rad} deduced from the line-integrals depends strongly on the knowledge of the energy resolved efficiency of the absorber. To this aim, the efficiency of the original Au-absorbers has been determined and proven to be close to unity in the wavelength range between $1\mu\text{m}$ and 1nm in case the absorbers have been blackened by using a coating to enhance the photon absorption in the visible range¹¹. Similar measurements have now been performed for the new prototype detectors, but the energy range investigated has significantly been extended towards high energies and the efficiency of absorbers of two different thicknesses were determined.

The efficiency of the bolometer prototypes could be measured in a very broad spec-

tral range (3 eV up to 25 keV) by making use of the synchrotron radiation facilities of the Physikalische Technische Bundesanstalt (PTB) at the electron storage rings BESSY II and Metrology Light Source (MLS). Additional measurements for the VIS (1.46 eV up to 3 eV) have been conducted in the lab. The characteristics of all measurement stations used, the corresponding experimental set-up and the data evaluation procedures are described in section II. The measurement results are described and discussed in section III. The results are compared to values for the expected reflectance and X-ray absorption of Pt. In particular the latter could be used to cross check the thickness of the absorber layer. Finally, section IV concludes with a focus on the applicability of the bolometer detector prototypes for the application in diagnostics of fusion devices.

II. EXPERIMENTAL SET-UP

A. Description of the measuring stations

For the efficiency calibration to cover the broad spectral range from 1.46 eV up to 25 keV, several measurement stations had to be used. The measurements in the energy range above 3 eV, respectively below 400 nm wavelength, were performed in the laboratory of the PTB making use of monochromatized synchrotron radiation provided by the electron storage rings BESSY II¹² and MLS¹³ in Berlin. Five beamlines were used: the VUV radiometry beamline¹⁴ and the EUV radiometry beamline¹⁵ at the MLS, and the soft X-ray radiometry beamline¹⁶, the four-crystal-monochromator beamline¹⁷, and the double-crystal monochromator at the BAMline¹⁸ at BESSY II.

A set-up for the measurements in the VIS (400 nm–850 nm) has been realised in the laboratory of IPP. A 250 mm Czerny-Turner spectrograph was used to split the spectrum of a halogen cold light source from Schott (Model KL1500 LCD) with a nominal output of 150 W. The resulting beam of light with a spectral width of 5.3 nm at 400 nm and 4.4 nm at 850 nm, respectively, was focused onto the detector surface by an assembly of lenses and apertures. The wavelength calibration of the spectrograph was checked using He, Ne, Hg, Zn, Cs and Kr spectral lamps. An accuracy of 0.4 nm was achieved. The detector was placed in a dedicated housing to shield it from stray light and influences due to convection. Additionally, three lasers with wavelengths of 405 nm, 532 nm and 635 nm, respectively, were

focused onto the detector to provide a few measurements with a high signal-to-noise ratio.

B. Description of the measurement procedures

At the measuring stations of the PTB, the bolometer detectors to be examined were investigated under vacuum conditions (except at the BAMline) by comparison to calibrated silicon photodiodes as reference detector. The photodiodes were calibrated in the respective spectral ranges against the cryogenic radiometers as primary detector standards of PTB^{19–21} so that the incident radiant power was determined for the present calibration with relative uncertainties of about 1%. The detectors were fastened to translation stages which allowed linear motion in two perpendicular directions. In this way it was possible to scan over the sensitive area of the detector by means of the X-ray beam. For every photon energy, the radiant power in the monochromatic beam was first measured by means of the reference detector. Then, the measurement of the detector to be calibrated was performed for different channels. At the end of each measurement cycle, the radiant power was measured once again by means of the reference detector in order to detect any instability that might have been caused, for example, by instabilities of the electron beam position.

For the measurements at the MLS (VUV and EUV radiometry beamlines) the storage ring was operated in the decaying mode, i.e. the stored current decreased with time. Therefore, the measured signal had to be normalized to the stored current at this time. The corresponding data on the stored current for the VUV beamline, respectively a reference signal for the EUV beamline were provided and taken into account during data evaluation. For the X-ray beamlines at BESSY II, the storage ring was operated in the top-up mode for most of the measurements, i.e. the stored current was kept constant and the radiant power did not vary. This was proven by the reference measurements. Only for some measurements at the BAMline, no top-up mode was achieved. The evaluation of these measurements took the decaying beam intensities into account using the measurements of an ionisation chamber operated in parallel as reference.

The measurements in the VIS range were performed in air. For each wavelength, the size of the light beam focused onto the detector was adjusted to fall completely onto the absorber area. Its intensity was determined before and after each calibration measurement using a calibrated X93 power meter from Gigahertz Optik. The relative calibration uncertainty of

the power meter is 5 %.

C. Description of the data acquisition and evaluation

For all calibration measurements the prototype detectors (bolometer 1: flow chart 1100025, wafer 481, chip L with $12.5\mu\text{m}$ thick absorber; bolometer 2: flow chart 900076, wafer 234, chip D with $4.5\mu\text{m}$ thick absorber) have been connected to the same data acquisition hardware. It consists of power supplies and bolometer amplifiers²² (one for each detector channel) with a 2 kHz square wave and an amplitude of $U_0 = 10\text{ V}$. They are connected to a PXI 7833R module from National Instruments and can be operated in both, calibration mode (to determine the detector parameters meander resistance R , cooling time constant τ , normalised heat capacity κ and offset of the Wheatstone-bridge U_{offs} in-situ) or measurement mode. The respective procedures have been described in detail elsewhere²³. The measurements can be performed using different sampling times (19.2 ms, 12.8 ms, 6.4 ms, 3.2 ms, 1.6 ms and 0.8 ms) and the 24bit ADC can be set to map various measurement ranges ($\pm 10\text{ mV}$, $\pm 20\text{ mV}$, $\pm 40\text{ mV}$, $\pm 80\text{ mV}$). The latter was chosen such that the bridge voltage to be measured including the offset optimally fits into the measurement range. The sampling time chosen for the experiments was the highest one in order to reduce readout noise as much as possible.

Before each measurement, the procedures for determining R , τ , κ and U_{offs} have been run. After acquiring the measurement signals, i.e. the time trace of the bridge voltage U_b for each detector channel, the detected power P_{rad} is evaluated according to equation 16 in reference²³

$$P_{\text{rad}} = A\kappa \left[\tau \frac{dU_b}{dt} + U_b \left(1 - \frac{B}{\kappa} \right) \right] \quad (1)$$

and a software implementation of the Savitski-Golay-filter for calculating the time derivative of U_b . The constants A and B depend on the properties of the electrical circuit for each Wheatstone bridge, e.g. R , U_0 , cable resistance, etc.

The power of the monochromatic radiation used for the efficiency calibration varied between $0.2\mu\text{W}$ and $50\mu\text{W}$, depending on the photon energy. These powers are for the most part significantly lower than those detected during experiments on fusion devices. Thus, to reduce uncertainties by evaluating time averaged signals, each measurement cycle was defined to last up to 30 s during which the beam illuminated the detector for 12 s by operating

a shutter synchronous to the data acquisition. Furthermore, after applying the measurement voltage onto the bolometer bridge, at least three measurement cycles have been acquired to allow for the detector to approach thermal equilibrium. Still, the offset drift was non-negligible in these cases and the background of the measurement signal showed variations which had to be taken into account for the evaluation.

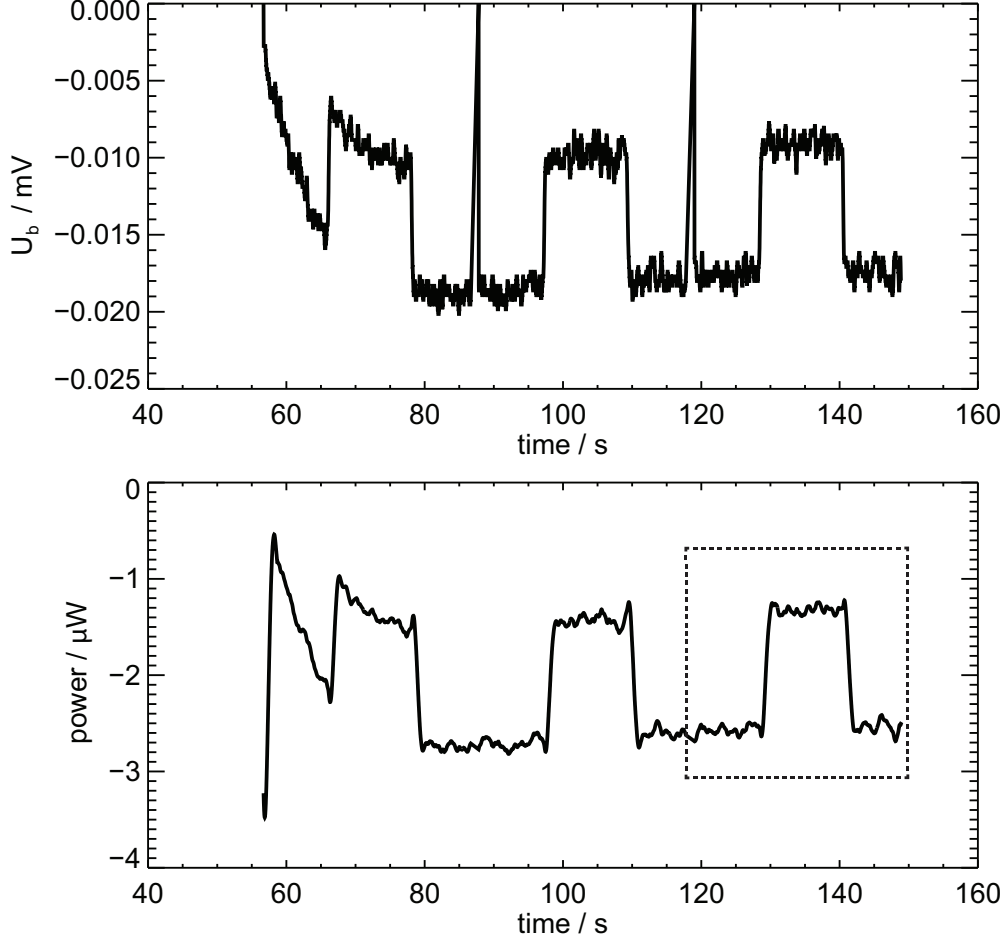


FIG. 1. Time trace of the bolometer measurement at 649 nm (bolometer 2, channel 1). Top: Bridge voltage U_b as measured for three cycles; Lower: Detected power for the three measurement cycles. The last cycle (dotted frame) is shown enlarged after offset correction in figure 2.

An example of such a time trace is shown in figure 1. On the top, the bridge voltage U_b for the complete time trace of the bolometer measurement with three cycles, taken during the calibration at 649 nm for bolometer 2, channel 1, can be seen. In the lower part, the power calculated from U_b is shown for these cycles. The last cycle, indicated by a dotted frame, is shown enlarged in figure 2. For all measurements made, the background can be

well approximated using a linear function. The parts of the time trace used to determine this function are indicated in blue. Subtracting this function from the signal yields the time trace shown in figure 2. The power as measured by the bolometer is now determined by

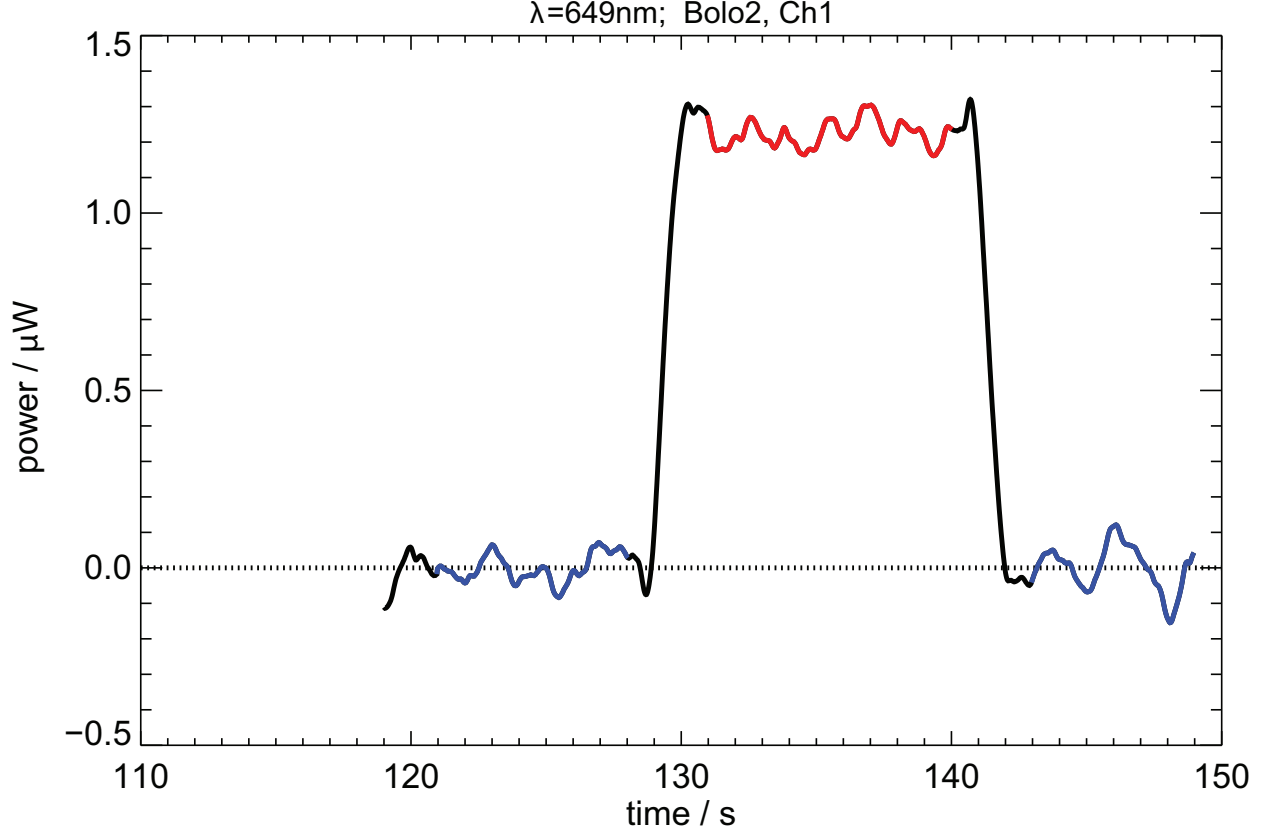


FIG. 2. Time trace of the detected power for the third cycle of the bolometer measurement for calibration at 649 nm (bolometer 2, channel 1), background subtracted.

calculating the average value of the signal during the time when the shutter was open. The respective parts of the time trace are marked in red. The number of time-steps will be denoted by N_t . Those parts of the time during which the shutter opens or closes, plus an additional delay to account for the filter width of the Savitzky-Golay-filter (also applicable at the start of the measurement cycle), have neither been used for calculating the background nor the average power (black parts of the time trace in figure 2). Note that this method excludes the transient times of U_b from the data evaluation. Therefore, the measured power P_{rad} is just proportional to U_b (equation 1).

The uncertainty of the calculated power is determined using Gaussian error propagation and taking all input uncertainties into account: The linear approximation of the background

yields the background function $y(t) = a + b \cdot t$ with the 1-sigma uncertainty estimates of the parameters, Δa and Δb , from the least squares fit. The power signal after background subtraction, $P(t) = P_{\text{rad}}(t) - y(t)$, with $P_{\text{rad}}(t)$ being the uncorrected signal as determined from the measurement of the bridge voltage according to equation 1, has the uncertainty $\Delta P(t) = \Delta a + \Delta b \cdot t$, the calculated average power on the bolometer, $P_{\text{bolo}} = \frac{1}{N_t} \sum_{t=1}^{N_t} P(t)$, has the uncertainty $\Delta P_{\text{bolo}} = \frac{1}{N_t} \sum_{t=1}^{N_t} (\Delta a + \Delta b \cdot t)$.

The efficiency η for each photon energy measured is thus

$$\eta = \frac{P_{\text{bolo}}}{P_0} \quad (2)$$

where P_0 is the radiant power, measured with calibrated diodes. The uncertainty $\Delta \eta$ of the efficiency is then given by

$$\Delta \eta = \sqrt{\left(\frac{\Delta P_{\text{bolo}}}{P_0}\right)^2 + \left(\frac{P_{\text{bolo}}}{P_0^2} \Delta P_0\right)^2} \quad (3)$$

with the uncertainty of the radiant power ΔP_0 .

III. DISCUSSION OF THE MEASUREMENT RESULTS

A. Scan of measurement frequency and range settings

In order to achieve optimal signal-to-noise ratios during the calibration measurements, the sampling time was set to 19.2 ms, the highest value possible for the ADC used. Additionally, the different settings for the signal range have been used to adapt to the offset of the Wheatstone-bridge during the experiment. In most cases a range setting of 20 mV was used, in a few cases 40 mV had to be applied. For assuring that these settings have no influence on the calibration result, scans have been performed at several photon energies.

Figure 3 shows the result of scanning the range setting. The efficiency of several bolometer channels has been determined at various photon energies (see legend in figure 3). The results match well within the uncertainties of the measurements. Furthermore, there is no clear correlation between the range setting and the resulting uncertainty of the measurement.

Similarly, the influence of the measurement sampling time has been investigated. Figure 4 shows the efficiency of several bolometer channels at various photon energies versus the sampling time. Clearly, the sampling time has no influence on the resulting efficiency, either.

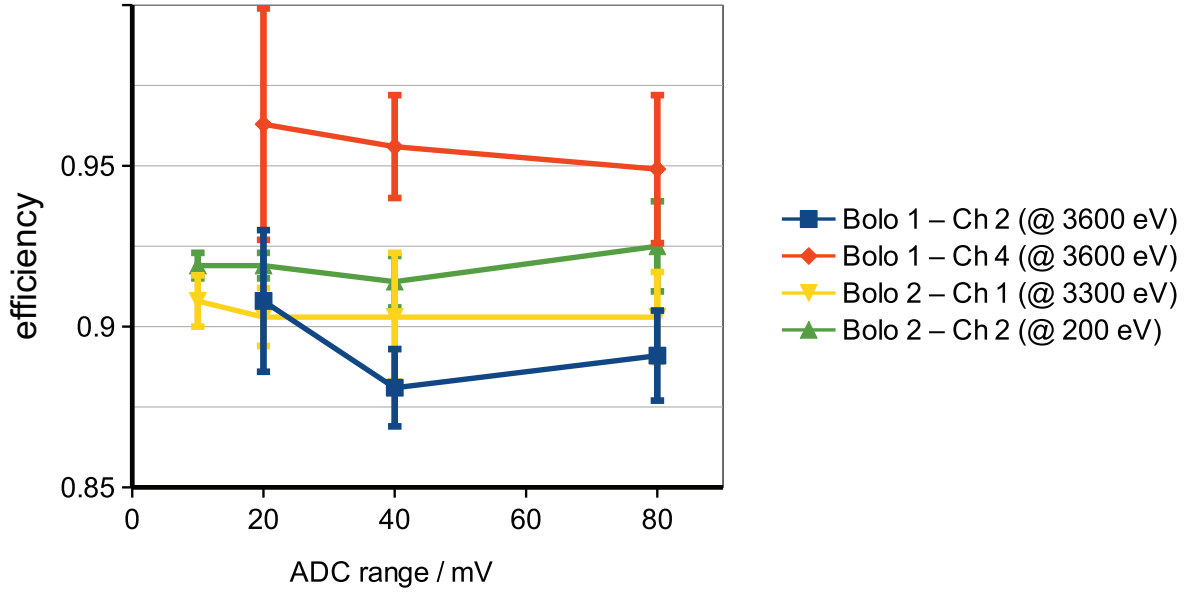


FIG. 3. Efficiency of 4 bolometer channels for various photon energies versus measurement range.

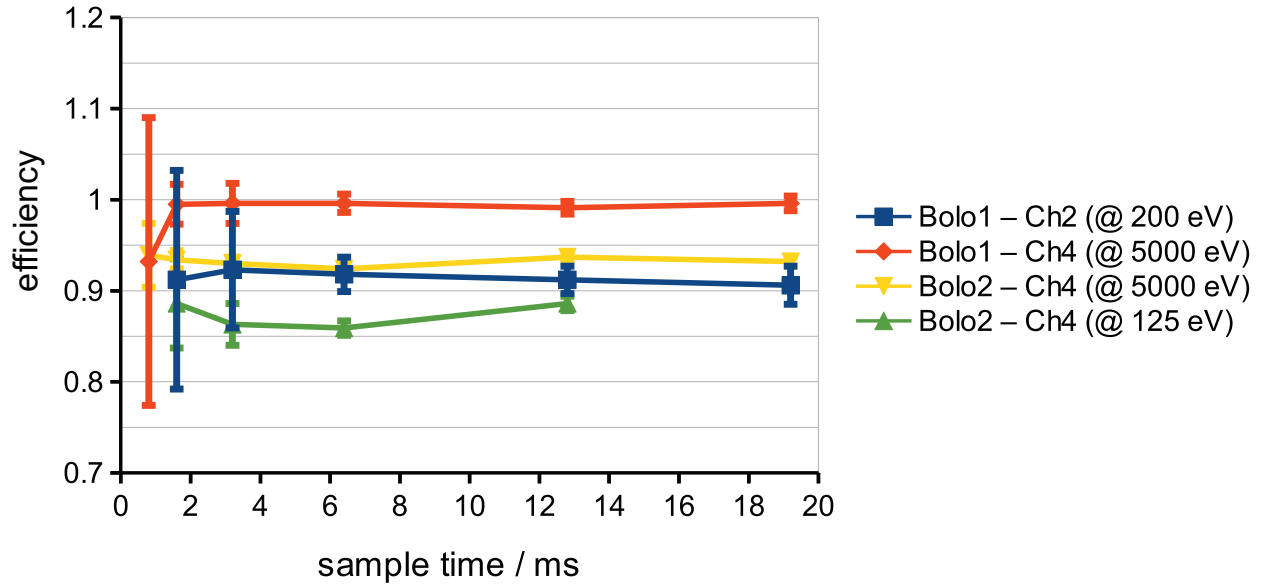


FIG. 4. Efficiency of 4 bolometer channels for various photon energies versus sampling time.

However, the lower the sampling time is, the higher are the uncertainties of the result. This can be expected as the thermal noise of the electronics is proportional to the square root of the bandwidth of the measurement and thus indirect proportional to the square root of the sampling time. As this applies to the measured signal, i.e. the bridge voltage U_b , the

uncertainties seen in figure 4 are additionally enhanced by the evaluation procedure and thus reflect this correlation only qualitatively.

B. Efficiency calibration

The efficiency of the two bolometer detector prototypes has been determined for channel 1 and 4 respectively over the energy range from 1.46 eV up to 25 keV, corresponding to a wavelength range from 850 nm up to 0.05 nm. Figure 5 shows all results within one graph. Efficiency values for bolometer 1 (thick absorber) are shown using diamonds, those of bolometer 2 (thin absorber) squares. For both bolometers values from channel 1 are given in blue, those of channel 4 in magenta. For some energies the efficiency has been determined also for the other channels (see e.g. figures 3 and 4) demonstrating that the variations from channel to channel are in the same ballpark as those shown.

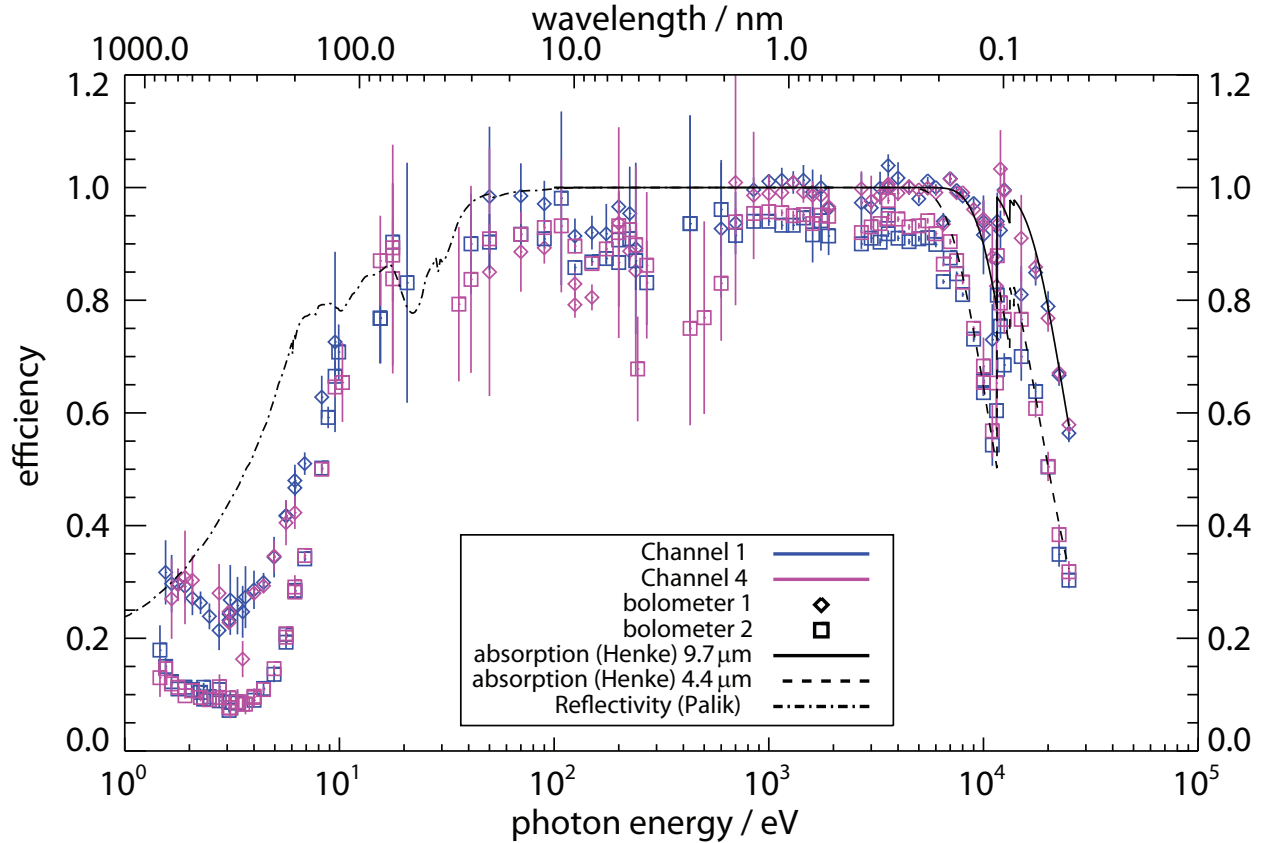


FIG. 5. Efficiency of 4 bolometer channels versus photon energy.

The radiant power of the incident beam used for calibration varied — according to the

characteristics of the respective measurement stations — between $0.2\ \mu\text{W}$ and $50\ \mu\text{W}$. For the measurements using the lasers in the VIS range intensities up to $6\ \text{mW}$ have been reached. In figure 5 the efficiency values with the highest uncertainties correlate to measurements which had to be made at the lowest radiant powers.

In addition to the efficiency values, the absorption coefficients according to Ref. 24 are drawn in figure 5 as a continuous line for an assumed Pt-thickness of $9.7\ \mu\text{m}$ and as a dashed line for an assumed Pt-thickness of $4.4\ \mu\text{m}$. For energies below $100\ \text{eV}$ the reflectivity of polychristalline Pt under 90° incidence according to Ref. 25, page 336, is drawn as a dot-dashed line. These values from literature denote the efficiency of the bolometers which could be expected in an ideal case.

The results obtained for the prototype bolometers with the thick absorber at photon energies above $200\ \text{eV}$ agree within the measurement uncertainties well with these expectations from literature. The efficiency obtained for the thin absorber also follows nicely the expectations from literature but shows slightly lower values.

For part of the VUV and the EUV spectral range ($20\ \text{eV}$ up to $250\ \text{eV}$), the efficiency values are slightly lower than expected from literature. But still they agree well enough within the measurement uncertainties. For energies lower than $10\ \text{eV}$, the efficiency of the bolometers is increasingly lower than expected and a systematically different behaviour can be observed for the two prototype detectors: while the efficiency of bolometer 1 is decreased by up to a factor of 2 with respect to the values expected from literature, the one for bolometer 2 is decreased by a factor of up to 4. The detectors have been produced in different batches and more than one year delayed in time. Additionally, they have been treated differently before performing these measurements, in particular they have been submitted to a different number of annealing cycles at different temperatures and in varying environments. Therefore, it is assumed that the absorber surfaces have developed slightly different passivation layers. As the photons in this energy range are absorbed close to the surface, it is assumed that the passivation layers are not thermally well coupled to the absorber and thus lead to different effective cooling time constants than determined by the ohmic calibration procedure and therefore result in the observed efficiencies.

Figure 6 shows the high energy spectrum of the efficiency values for bolometer 2 enlarged and on a linear photon energy scale. The absorption coefficients from literature²⁴ have been used to fit them to the measured values by using the thickness of the absorbing layer as

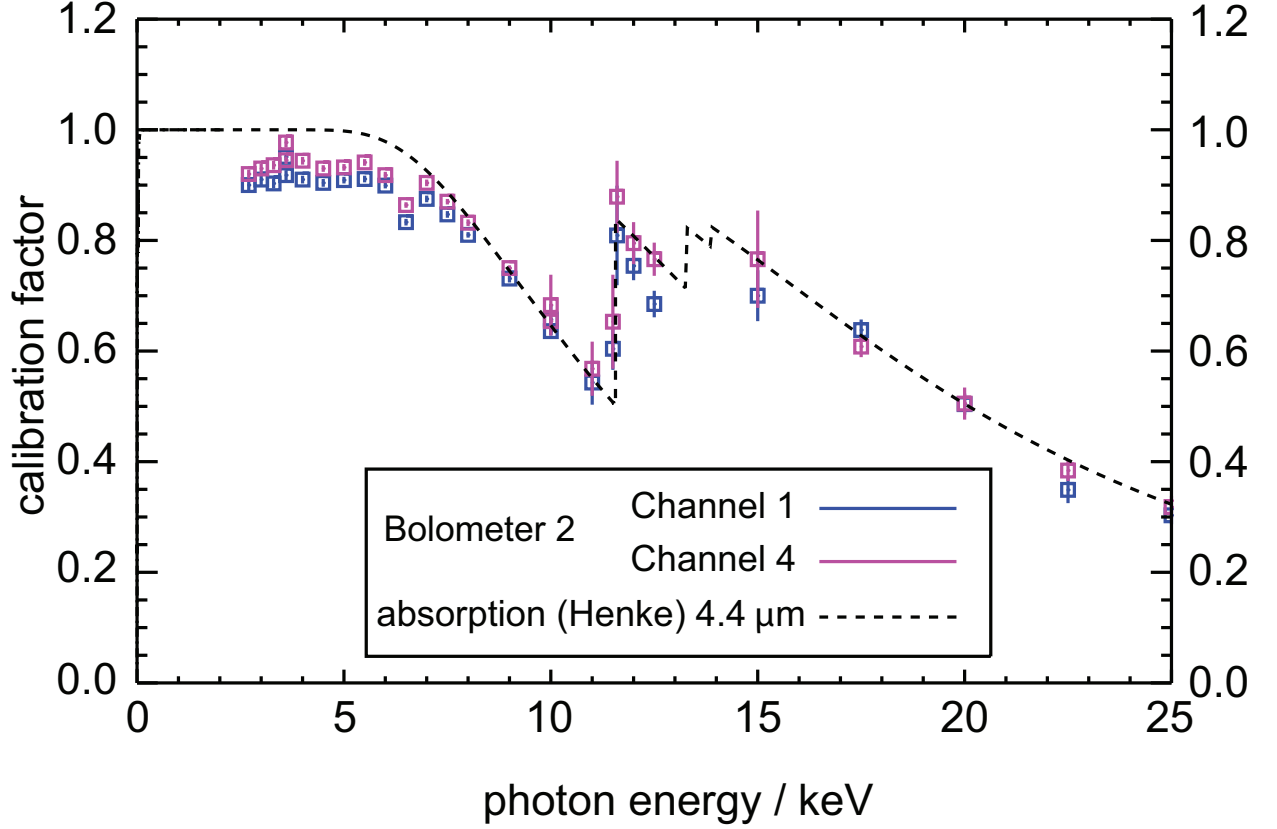


FIG. 6. Fit using absorption coefficient data from literature to calibration results of bolometer 2 (thin absorber).

the only free parameter and assuming it to be homogeneous. The sharp Pt- L_3 absorption edge at 11.56 keV is excellently suited to constrain the fit. The result demonstrates that a Pt-thickness of $4.4\ \mu\text{m}$ (with an uncertainty of the fit of $\pm 0.15\ \mu\text{m}$) is in very good agreement with the measurement results and corresponds well to the nominal thickness of $4.5\ \mu\text{m}$ from the manufacturing process. Additionally, absorber thicknesses were measured using Rutherford-backscattering (RBS)²⁶ with 3.5 MeV incident protons at a scattering angle of 165° at the tandem accelerator of IPP Garching. The measured energy spectra were converted to depth profiles using the SIMNRA program²⁷ with SRIM-2003 stopping powers resulting in a value of $(4.4 \pm 0.1)\ \mu\text{m}$.

Figure 7 shows the corresponding result for bolometer 1. In this case, the best fit of the absorption coefficient literature data yields a Pt-absorber with a thickness of $(9.7 \pm 0.3)\ \mu\text{m}$. This is significantly lower than the nominally expected values of $12.5\ \mu\text{m}$ from the manufacturing process. Even when taking nonuniformities of the electroplating process over

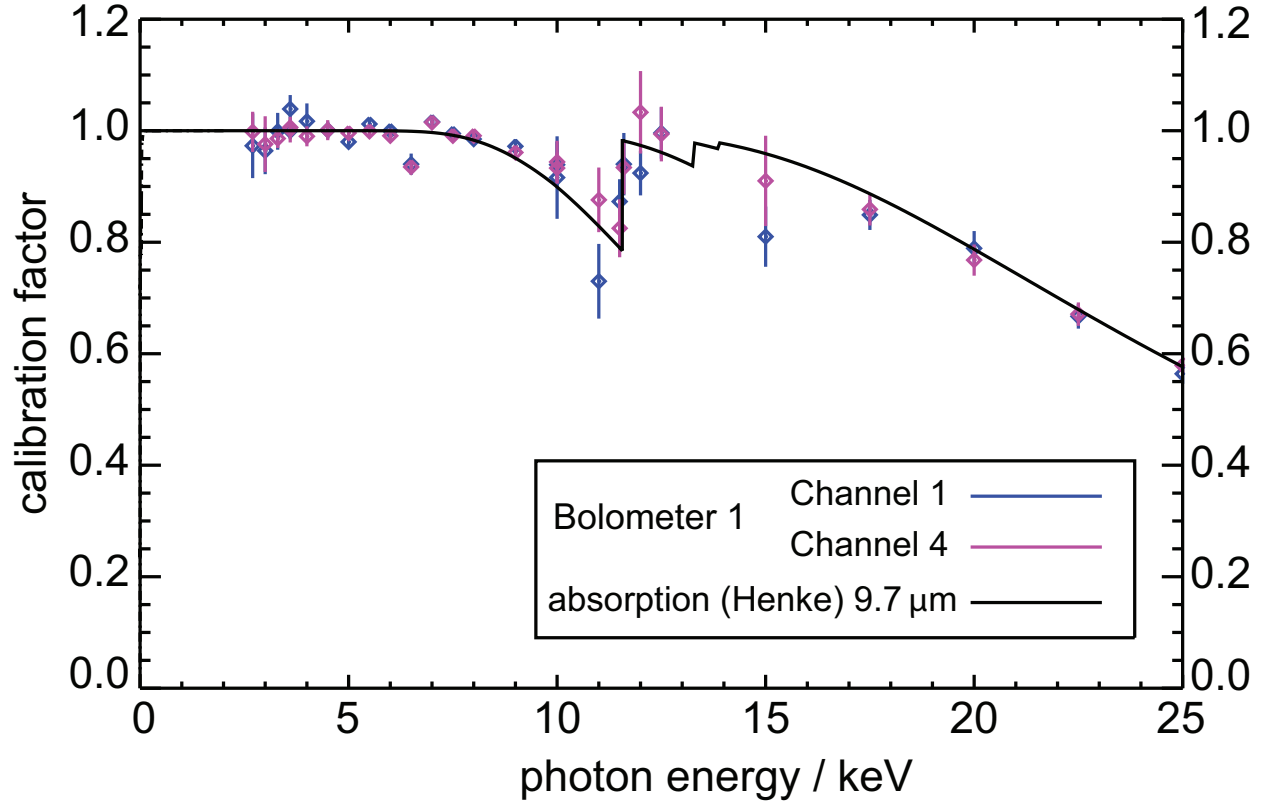


FIG. 7. Fit using absorption coefficient data from literature to calibration results of bolometer 1 (thick absorber).

the wafer (which contained 16 individual detectors) into account, the Pt-thickness is not expected to be lower than $11.75\ \mu\text{m}$. For the prototypes with thick absorber the RBS measurements still have to be carried out. They will confirm if the nominal thickness from the production process is correct or not, or if the density of the Pt-layer differs from the standard literature conditions of $21.4\ \text{g}/\text{cm}^3$, which were used in the evaluation.

C. Lowest detectable signal level

According to figure 2 the power as determined by bolometer 2 ($4.5\ \mu\text{m}$ absorber) has a noise level of $\pm 0.1\ \mu\text{W}$; the one for bolometer 1 ($12.5\ \mu\text{m}$ absorber, not shown as graph) has a noise level of $\pm 0.2\ \mu\text{W}$. Thus, under optimal conditions (i.e. steady-state conditions and long sampling time), the lowest power level which can be detected by the bolometers is about $0.2\ \mu\text{W}$. Taking the surface area of the detector exposed to the radiation of $1.3\ \text{mm} \times 3.8\ \text{mm} = 4.94 \cdot 10^{-6}\ \text{m}^2$ into account, this relates to a line averaged radiant power density of $40\ \text{mW}/\text{m}^2$

which would be the lower limit detectable in a fusion experiment when using these detectors.

However, as stated above, this is valid only for optimal conditions. For time resolved measurements, additional uncertainties arise from the time derivative of U_b in the evaluation of the radiant power. Furthermore, even after thermal equilibration of the detector assembly, drifts of the background, which might rise up to $10\ \mu\text{V}$ ($\approx 3\ \mu\text{V}$ in figure 1, top), have to be taken into account. Thus, the lowest radiant power detectable in time resolved measurements will be in the order of $1\ \mu\text{W}$, relating to a line averaged radiant power density of $0.2\ \text{W}/\text{m}^2$. This compares well to a first performance analysis of a proposed LOS arrangement for ITER²⁸, which indicates expected signal levels between $4\ \text{W}/\text{m}^2$ and $2300\ \text{W}/\text{m}^2$ in the ITER standard scenario, depending on the properties of the LOS. Still, as plasma radiation needs to be measured in ITER also during other scenarii, in particular during plasma start-up with lower overall radiation levels, some lines-of-sight will need additional optimisation to enhance the light yield so that their signal-to-noise ratio will be acceptable. Also, improvements in the electronics need to be considered as well as their optimal adaptation to the detector thickness chosen and the time resolution requested.

IV. CONCLUSIONS

The energy resolved efficiency of two bolometer detector prototypes with 4 channels each and nominal absorber thicknesses of $4.5\ \mu\text{m}$ and $12.5\ \mu\text{m}$, respectively, has been calibrated in a broad spectral range from $1.46\ \text{eV}$ up to $25\ \text{keV}$ (corresponding to $850\ \text{nm} - 0.05\ \text{nm}$) making use of a dedicated experimental set-up for the VIS range in the laboratory and the facilities of the PTB on the electron storage rings MLS and BESSY II for the energy range above $3\ \text{eV}$.

The results from scanning range and sampling time settings demonstrated that the data acquisition system used to implement the in-situ calibration procedure and the measurements is well capable of applying various range and sampling time settings which can be chosen to match the experimental conditions. Measuring low incident intensities helped to assess the performance of the prototype detectors and to project this to the use on a fusion experiment like ITER. It could be shown that, depending on the settings for the sampling time, line averaged radiation intensities of as low as $0.2\ \text{W}/\text{m}^2$ can be detected by these bolometer prototypes.

The calibration measurements clearly demonstrate that the efficiency of the bolometer prototype detectors in the range of 50 eV up to ≈ 6 keV is close to unity; at a photon energy of 20 keV the thick absorber detects 80% of the photons, the thin absorber about 50%. This indicates that the detectors will be well capable of providing an absolutely calibrated measurement of the plasma radiation expected from the standard ITER scenario. However, a minimum thickness, which can be determined by using literature data for the absorption coefficient of the absorber material, will be required to detect the high energetic radiation from the central plasma.

At 11.56 keV the sharp Pt-L₃ absorption edge allowed to cross-check the absorber thickness by fitting the measured efficiency to the theoretically expected absorption of X-rays in a homogeneous Pt-layer. The nominal thickness of the thin absorbers could be confirmed, however not the one of the thick absorbers. To decide whether the discrepancies between nominal and measured thickness are due to differences in the assumed Pt-density of the absorber or variations in the production process, RBS measurements will be performed.

Furthermore, below 50 eV the photon absorption first follows the reflectance expected for Pt, but below 10 eV it is reduced further by a factor of 2 for the thick absorber and a factor of 4 for the thin absorber. Most probably, the different histories in production, storage and operation led to varying surface conditions which in turn influence the loss channels. For future detector prototypes it is envisaged to investigate possibilities for blackening the absorber in order to enhance the photoabsorption in the VIS and VUV range. However, in view of ITER it will be highly important to consider potential degradation effects due to such measures.

ACKNOWLEDGMENTS

The authors are grateful to M. Mayer for performing and evaluating the RBS measurements and to A. Sigalov for his invaluable assistance in setting up the data acquisition system.

The work presented herein has been funded by the German Federal Ministry of Education and Research (grant 03FUS0006). The sole responsibility for the contents of this publication lies with the author.

REFERENCES

- ¹K. F. Mast, J. C. Vallet, C. Andelfinger, P. Betzler, H. Kraus, and G. Schramm. A low noise highly integrated bolometer array for absolute measurement of VUV and soft-X radiation. *Review of Scientific Instruments*, 62(3):744–750, 1991.
- ²H. Meister, L. Giannone, L.D. Horton, G. Raupp, W. Zeidner, G. Grunda, S. Kalvin, U. Fischer, R. Reichle, A. Serikov, and S. Stickel. The ITER bolometer diagnostic - status and plans. *Review of Scientific Instruments*, 79:10F511–1 – 10F511–5, 2008.
- ³K. McCormick, A. Huber, C. Ingesson, F. Mast, J. Fink, W. Zeidner, A. Guigon, and S. Sanders. New bolometry cameras for the JET Enhanced Performance Phase. *Fusion Engineering and Design*, 74:679–683, 2005.
- ⁴A. W. Leonard, W. H. Meyer, B. Geer, D. M. Behne, and D. N Hill. 2D tomography with bolometry on DIII-D. *Review of Scientific Instruments*, 66(2):1201–1204, 1995.
- ⁵B J Peterson, A Yu Kostrioukov, N Ashikawa, Y Liu, Yuhong Xu, M Osakabe, K Y Watanabe, T Shimosuma, S Sudo, and the LHD Experiment Group. Bolometer diagnostics for one- and two-dimensional measurements of radiated power on the large helical device. *Plasma Physics and Controlled Fusion*, 45(7):1167, 2003.
- ⁶M. Gonzalez and E. R. Hodgson. Electrical and mechanical behaviour of improved platinum on ceramic bolometers. *fed*, 82:1277–1281, 2007.
- ⁷H. Meister, T. Eich, N. Endstrasser, L. Giannone, M. Kannamüller, A. Kling, J. Koll, T. Trautmann, P. Detemple, and S. Schmitt. Optimization of a bolometer detector for ITER based on Pt absorber on SiN membrane. *Review of Scientific Instruments*, 81:10E132, 2010.
- ⁸H. Meister, M. Kannamüller, J. Koll, A. Pathak, F. Penzel, T. Trautmann, P. Detemple, S. Schmitt, and H. Langer. Reliability issues for a bolometer detector for ITER at high operating temperatures. *Review of Scientific Instruments*, 83:10D724, 2012.
- ⁹L. C. Ingesson, B. Alper, B. J. Peterson, and J.-C. Vallet. Tomography diagnostics: Bolometry and soft-x-ray detection. In A. E. Costley and D. W. Johnson, editors, *Special issue on plasma diagnostics for magnetic fusion research*, volume 53, chapter 7. Fusion Science and Technology, 2008.
- ¹⁰A. Kallenbach, M. Bernert, T. Eich, J.C. Fuchs, L. Giannone, A. Herrmann, J. Schweinzer, W. Treutterer, and ASDEX Upgrade Team. Optimized tokamak power exhaust with

- double radiative feedback in asdex upgrade. *Nuclear Fusion*, 52(12):122003, 2012.
- ¹¹P. T. Lang and K. F. Mast. Photoresponse of a miniaturized ultrabroad-band low-noise metal-film bolometer detector array. *J. Optics*, 27(1):25–29, 1996.
- ¹²B. Beckhoff, A. Gottwald, R. Klein, M. Krumrey, R. Müller, M. Richter, F. Scholze, R. Thornagel, and G. Ulm. A quarter-century of metrology using synchrotron radiation by PTB in Berlin. *Physica Status Solidi B — Basic Solid State Physics*, 246(7):1415–1434, JUL 2009.
- ¹³A. Gottwald, R. Klein, R. Müller, M. Richter, F. Scholze, R. Thornagel, and G. Ulm. Current capabilities at the Metrology Light Source. *Metrologia*, 49:S146–S151, 2012.
- ¹⁴A. Gottwald, U. Kroth, M. Richter, H. Schoeppe, and G. Ulm. Ultraviolet and vacuum-ultraviolet detector-based radiometry at the Metrology Light Source. *Measurement Science & Technology*, 21(12):125101, 2010.
- ¹⁵C. Laubis, A. Fischer, and F. Scholze. Extension of PTB’s EUV metrology facilities. In *Proc. SPIE 8322, Extreme Ultraviolet (EUV) Lithography III, 832236 (March 29, 2012)*, pages 832236–832236–9, 2012.
- ¹⁶F Scholze, G Brandt, P Muller, B Meyer, F Scholz, J Tummler, K Vogel, and G Ulm. High-accuracy detector calibration for EUV metrology at PTB. In *Proc. SPIE*, volume 4688, pages 680–689. SPIE; Semiconductor Equipment & Mat Int; International SEMATECH, 2002. Conference on Emerging Lithographic Technologies VI, SANTA CLARA, CA, MAR 05-07, 2002.
- ¹⁷M. Krumrey and G. Ulm. High-accuracy detector calibration at the PTB four-crystal monochromator beamline. *Nuclear Instruments and Methods in Physics Research Section A: Accelerators, Spectrometers, Detectors and Associated Equipment*, 467-468, Part 2:1175–1178, 2001.
- ¹⁸W. Görner, M.P. Hentschel, B.R. Müller, H. Riesemeier, M. Krumrey, G. Ulm, W. Diete, U. Klein, and R. Frahm. BAMline: the first hard X-ray beamline at BESSY II. *Nuclear Instruments and Methods in Physics Research Section A: Accelerators, Spectrometers, Detectors and Associated Equipment*, 467-468, Part 1:703–706, 2001.
- ¹⁹A. Gottwald, U. Kroth, M. Krumrey, M. Richter, F. Scholze, and G. Ulm. The PTB high-accuracy spectral responsivity scale in the VUV and X-ray range. *Metrologia*, 43(2):S125, 2006.
- ²⁰M Gerlach, M Krumrey, L Cibik, P Müller, H Rabus, and G Ulm. Cryogenic radiometry

- in the hard X-ray range. *Metrologia*, 45(5):577, 2008.
- ²¹F Scholze, J Tümmler, and G Ulm. High-accuracy radiometry in the EUV range at the PTB soft X-ray beamline. *Metrologia*, 40(1):S224, 2003.
- ²²L. Giannone, D. Queen, F. Hellman, and J. C. Fuchs. Prototype of a radiation hard resistive bolometer for ITER. *Plasma Physics and Controlled Fusion*, 47:2123–2143, 2005.
- ²³L. Giannone, K. F. Mast, M. Schubert, NBI Team, ECRH Team, and W7-AS Team. Derivation of bolometer equations relevant to operation in fusion experiments. *Review of Scientific Instruments*, 73(9):3205–3214, 2002.
- ²⁴B.L. Henke, E.M. Gullikson, and J.C. Davis. X-ray interactions: Photoabsorption, scattering, transmission, and reflection at $e = 50\text{--}30.000\text{ eV}$, $z = 1\text{--}92$. *Atomic Data and Nuclear Data Tables*, 54(2):181 – 342, 1993.
- ²⁵E. D. Palik, editor. *Handbook of Optical Constants of Solids*. Academic Press, 1997.
- ²⁶Y. Wang and M. Nastasi, editors. *Handbook of Modern Ion Beam Materials Analysis*, Warrendale, Pennsylvania, USA, 2009. Materials Research Society.
- ²⁷M. Mayer. SIMNRA user’s guide. Technical Report IPP 9/113, Max-Planck-Institut für Plasmaphysik, Boltzmannstr. 2, 85748 Garching, Germany, 1997.
- ²⁸S Kalvin and G. Grunda. Diagnostic design for ITER: Optimisation of the ITER bolometer lines-of-sight, performance analysis and engineering and design activities. Technical report, Final report to EFDA contract 06-1447 (TW6-TPDS-DIADES-5.2), Association EURATOM-HAS, 2008.